PB 214 287
DOT HS-820 211

OCCUPANT MOTION SENSORS: ROTATIONAL ACCELEROMETER DEVELOPMENT

Contract No. DOT-TSC-NHTSA-72-1
April 1972
Technical Report

U.S. DEPARTMENT OF TRANSPORTATION
NATIONAL HIGHWAY TRAFFIC SAFETY ADMINISTRATION
WASHINGTON, D.C. 20590

The opinions, findings, and conclusions expressed in this publication are those of the authors and not necessarily those of the National Highway Traffic Safety Administration.

1. Report No. DOT-HS-820-211	2. Government Accession No.	3. Recipient's Catalog No. PB 212 257
4. Title and Subtitle OCCUPANT MOTION SENSORS: ROTATIONAL ACCELEROMETER DEVELOPMENT		5. Report Date April 1972
		6. Performing Organization Code TIF
7. Author(s) A. Warner, D. Ofsevit, G. Plank		8. Performing Organization Report No. DOT-TSC-NHTSA-72-1
9. Performing Organization Name and Address U.S. Department of Transportation National Highway Traffic Safety Admin Washington, D.C. 20590		10. Work Unit No. 11. Contract or Grant No. 72-HS-05 13. Type of Report and Period Covered Technical Report
12. Sponsoring Agency Name and Address U.S. Department of Transportation National Highway Traffic Safety Admin Washington, D.C. 20590		14. Sponsoring Agency Code
15. Supplementary Notes Details of illustrations in this document may be better studied on microfiche		

16. Abstract

A miniature mouthpiece rotational accelerometer has been developed to measure the angular acceleration of a head during vehicle crash or impact conditions. The device has been tested in the laboratory using a shake table and in the field using dummies and humans. The results of the testing show that while the accelerometer is sensitive to angular acceleration it is also sensitive to linear acceleration, and in practical applications a correction factor for linear accelerations must be applied to the rotational output.

17. Key Words Acceleration, Accelerometer, Angular, Mouthpiece, Occupant Motion, Restraint System	18. Distribution Statement unlimited		
19. Security Classif. (of this report) Unclassified	20. Security Classif. (of this page) Unclassified	21. No. of Pages 343	22. Price

PREFACE

The work described in this report was performed as a part of the Occupant Motion Sensor Program initiated and sponsored by the National Highway Traffic Safety Administration. The programs principal objective is to develop practical instrumentation to accurately acquire occupant positional information during a vehicle crash or simulated crash and devise optimum methods to process this information

A secondary objective of the program is the measurement of head angular acceleration during crash conditions.

A significant amount of the experimental work described in this report was performed with the assistance of the personnel of the Crew Systems Division of the Naval Air Development Center and the Daisy Decelerator located at Holloman AFB. We wish to thank in particular M. Katzeff and M. Schulman of NADC/CSD and Major H. Russell of Holloman AFB.

TABLE OF CONTENTS

LIST OF ILLUSTRATIONS

1.0 INTRODUCTION

1.1 OBJECTIVE

The objective of the Occupant Motion Sensor project at TSC is to develop practical instrumentation to accurately measure human, animal or dummy motions during a vehicle crash. Since rapid deceleration of the head can cause brain injury, head acceleration is usually monitored during restraint systems testing. Off-the-shelf linear accelerometers are commonly used to measure the linear acceleration. The other component of head acceleration, rotational acceleration, however, is much more difficult to measure and is not currently being measured by field crash investigators. For this reason TSC is developing a miniature mouthpiece rotational accelerometer. This report describes this accelerometer and data obtained with it.

1.2 BACKGROUND

During FY71 an analysis and trade-off study was performed, a list of five promising systems for obtaining body kinematic measurements was developed and prototype systems were built and evaluated.* During the first part of FY72 a major effort was directed to the further development of one of the five systems, the mouthpiece rotational accelerometer. The effort was concentrated on the development of this device because the need for a rotational accelerometer is great and fabrication of the device appears to be possible using readily available components.

The prototype system was calibrated in the laboratory using a shaker table and pivoting arm arangement to produce angular accelerations. The device's output as a function of rotational acceleration was recorded. The first field tests were conducted using the NADC test sled at the Philadelphia Navy Yard. The accelerometer was mounted on a dummy head which rotated forward as the sled was accelerated. The second field tests were conducted at Holloman

*DOT-TSC-NHTSA-71-4 section 3

AFB, New Mexico. These tests employed human subjects using lap belt restraints. The results of the calibration and field tests are presented in this report.

2.0 ACCELEROMETER DESCRIPTION

The rotational accelerometer consists of two linear accelerometers with parallel sensitive axes separated by a known distance. The outputs are summed to produce rotational information (Section 3.0). The linear accelerometers are of the piezoelectric type which are small, light weight, rugged and have good high frequency response. As the name implies a piezoelectric accelerometer utilizes the piezoelectric effect. When a piezoelectric material such as quartz is subjected to a mechanical stress or deformation it generates an electric charge. In an accelerometer the piezoelectric material is used to support a seismic mass. Under an acceleration the mass cuases the support to distort thus producing a charge. The charge, which is proportional to the acceleration, is then processed by signal conditioning electronics and recorded.

Figure 1 shows the accelerometer with its output cable and connector. The device is small enough to be molded into a

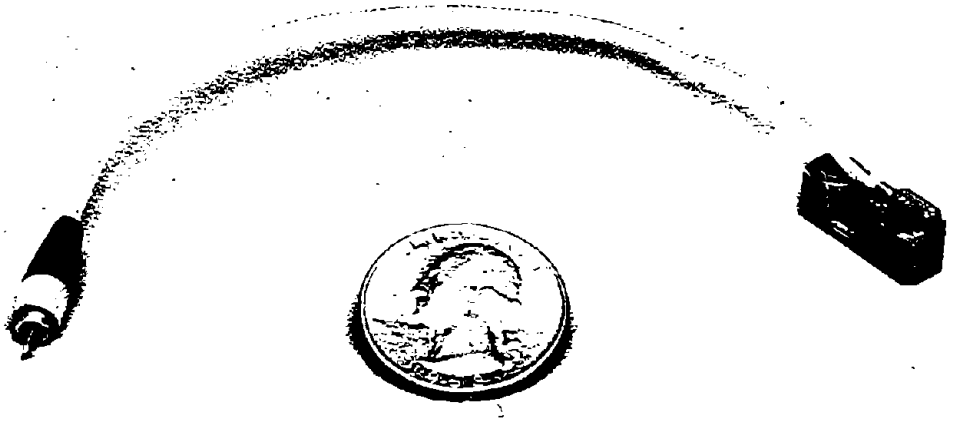

Figure 1. TSC Rotational Accelerometer.

mouthpiece which is then held in the subject's teeth. This ensures good mechanical coupling to the subject's head. The six-inch long flexible Microdot cable is routed forward between the subject's lips and out of his mouth to a longer cable and the signal processing electronics. Detailed specifications are listed below.

Size	.27"x.36"x.77"
Weight	5 grams
Sensitivity	.007pc/rad/sec^2
Linearity	1%
Maximum Acceleration	1000 g
Frequency Response	1.5Hz to 4kHz
Environmental	hermetic seal
Temperature Range	- 100°F to 350°F

3.0 LABORATORY EVALUATION

To determine the response characteristics of the rotational accelerometer, a complete laboratory evaluation was performed.

While the accelerometer was designed to measure pitch accelerations, a human or dummy in a crash situation will experience both linear and rotational accelerations. Therefore the transducer output due to linear accelerations and rotational accelerations that are not in the pitch plane must be determined. If the signals due to these motions are significant, they must be accounted for.

3.1 CALIBRATION (GENERAL)

Theoretically, rotational acceleration can be measured directly by the proper arrangement of two linear accelerometers.* These accelerometers are placed with their sensitive axes parallel to one another at some separation, d. Rotational acceleration about some point is given by the relationship:

$$\ddot{\theta} = \frac{\ddot{r}_1 - \ddot{r}_2}{d}$$

where $\ddot{\theta}$ = rotational acceleration

$\ddot{r}_1$, $\ddot{r}_2$ = linear acceleration of accelerometers 1&2 respectively along their sensitive axes.

d = distance between the accelerometers

The rotational acceleration measured is independent of the radius of curvature of the motion.

In order for the real situation to obey the theory, the two linear accelerometers must have their sensitivities perfectly matched. In the event of a mismatch, the device will also respond to any linear accelerations that might be present. Because of the

*Report No. DOT-TSC-NHSB-71-1, Appendix C.

difficulty in matching two linear accelerometers on their sensitive axes as well as their non-sensitive axes, the actual device will respond to linear accelerations and rotational accelerations about supposedly non-sensitive axes. Taking these responses into account the output of the device is of the form (see Appendix A):

$$Q_{out}\ (\text{picocoulombs}) = a\ddot{\theta}_x + b\ddot{\theta}_y + c\ddot{\theta}_z + d\ddot{x} + e\ddot{y} + f\ddot{z}$$

Consisting of three rotational components and three linear components. (Figure 2)
In the ideal case:

$$Q_{out} = a\ddot{\theta}_x$$

This is not the case however and the problem remains to determine the magnitude and sign of all the coefficients.

3.2 DETERMINATION OF COEFFICIENTS:

The coefficients of the Linear components of acceleration are found by vibrating the divice linearly along each axis. The

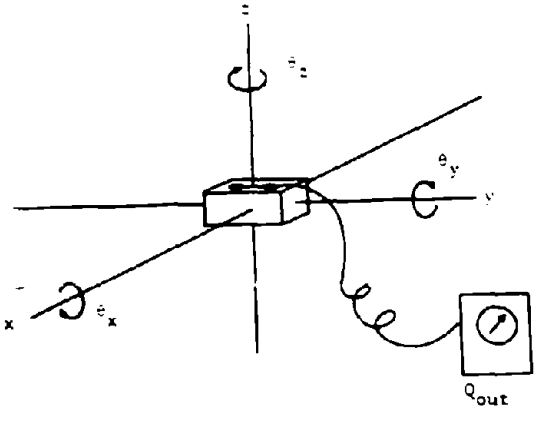

$Q_{out} = a\ddot{\theta}_x + b\ddot{\theta}_y + c\ddot{\theta}_z + d\ddot{x} + e\ddot{y} + f\ddot{z}$

a = .0068 PICOCOULOMBS/RADIAN/SEC^2
b = -.0003 "
c = .0000 "
d = .18 PICOCOULOMBS/G
e = .06 "
f = .09 "

Figure 2. Accelerometer Output for all Motions

coefficeints for accelerometer #002 were found to be:

$$d = .18 \text{ picocoulombs / g}$$
$$e = .06 \text{ picocoulombs / g}$$
$$f = .09 \text{ picocoulombs / g}$$

The coefficients of the rotational components were determined using a shake table and pivoting arm apparatus (described in Appendix A). The coefficients of the rotational components were found to be:

$$a = .0068 \text{ picocoulombs / rad / sec}^2$$
$$b = -.0003 \text{ picocoulombs / rad / sec}^2$$
$$c = .0000 \text{ picocoulombs / rad / sec}^2$$

Therefore, for this accelerometer we have:

$$Q_{out} \text{ (picocoulombs)} = .0068\,\ddot{\theta}_x - .0003\,\ddot{\theta}_y + .18\ddot{x} + .06\ddot{y} + .09\ddot{z}$$

By monitoring the magnitudes of the linear components and spurious rotational components, a very accurate measure of the angular acceleration about the x axis, $\ddot{\theta}_x$, can be obtained.

4.0 FIELD TESTS (DUMMIES)

The first field tests of the piezoelectric rotational accelerometer system were conducted using the catapult facility at the Johnsville Naval Air Development Center to validate the accelerometer performance. The test configuration consisted of a instrumented athropometric dummy head coupled to the sled by a hinge at the neck (Figure 3). During the test a square acceleration pulse (nominally 5g) was applied to the sled, and the head was allowed to rotate around the hinge through a 90 degree angle until the chin hit a stop. Instrumentation on the sled included the TSC rotational accelerometer, a second rotational accelerometer supplied by the Navy, a rate gyro, and high speed cameras. In addition, the sled's linear acceleration was measured. Figure 4 is a photograph of the dummy head. The black bar on the top of the head holds both the miniature rotational accelerometer (middle of the bar) and two linear accelerometers (ends of the bar). The

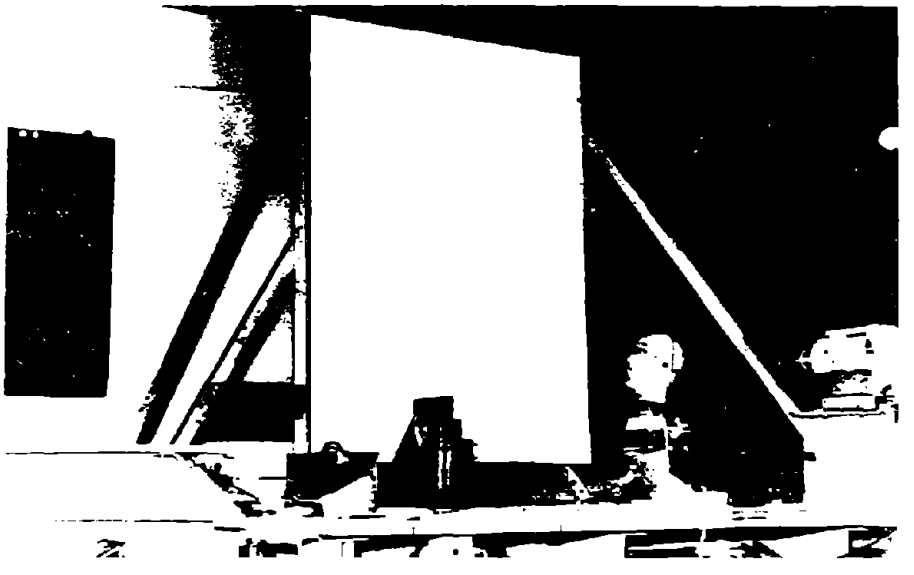

Figure 3. NADC Test Configuration

Figure 4. NADC Dummy Head

outputs of the linear accelerometers are electronically combined to give a voltage which is proportional to angular acceleration. The rate gyro is mounted inside the head and its lead can be seen coming out between the dummy's eyes. The motion of the head can be damped by adjusting the large nut and friction washers located at the neck. Thus each of the three rotational properties of motion were measured directly. The cameras recorded the head's angular position, θ, as a function of time. The rate gyro measured the head's angular velocity, $\dot{\theta}$, as a function of time and the accelerometers measured the angular acceleration, $\ddot{\theta}$, as a function of time. The output of any instrument could be verified by either integrating or differentiating the output of another instrument. Figure 5 shows the three directly-measured properties of motion for one run.

High-speed photographs taken at 1000 frames per second were scanned by a film reader to provide data that the computer could use. As it presently exists, the film reader requires that the

operator project one frame of film at a time and line up a cursor with whatever marker was used on the subject. The cursor is attached to a precision rotary potentiometer which converts the angle, θ, to voltage. This voltage is read by a digital voltmeter, which records the value on a small printer. The operator must then use a teletype terminal to transcribe this printed data onto punched paper tape which the computer can read.

The high-speed film data for these runs was satisfactory for two reasons. First, the camera was mounted on the sled and the dummy head had a fixed center of rotation, so that the motion on the film was almost all rotational with little translation. Second, the camera was close enough to the dummy head so that the mark used to align the cursor was large and clear. Still, the data contained some noise and it was necessary to filter the data. The Fast Fourier Transform* and Gaussian filter** computer programs were used to provide a half-power point of approximately 50Hz. This is a relatively small amount of filtering, when compared to that needed for live-subject tests. (See Section 5) This filtered data is plotted in Figure 5.

The rate gyro and rotational accelerometer data were recorded on magnetic tape. Because much of the data of interest occurs in the lower frequency band (20 Hz or less), an FM tape recorder is used. Such a recorder does not have the low frequency limitation of a direct-channel recorder. The recorded data was fed to an analog-to-digital converter which took 3500 samples/sec and stored them on computer magnetic disc in digital form. This sampling rate yielded a system bandwidth of 1750 Hz, which is greater than that of any expected data in this project.*** Once the data are stored, the computer can process it. It was not necessary to filter the data from magnetic tape; here the computer was used to scale the data (by taking samples of calibration signals) and to plot the processed data. All the signal plots in this report are reproduced

*Report No DOT-TSC-NHTSA-71-4, Section 4.1.
**Ibid, p. 31.
***Ibid, p. 29

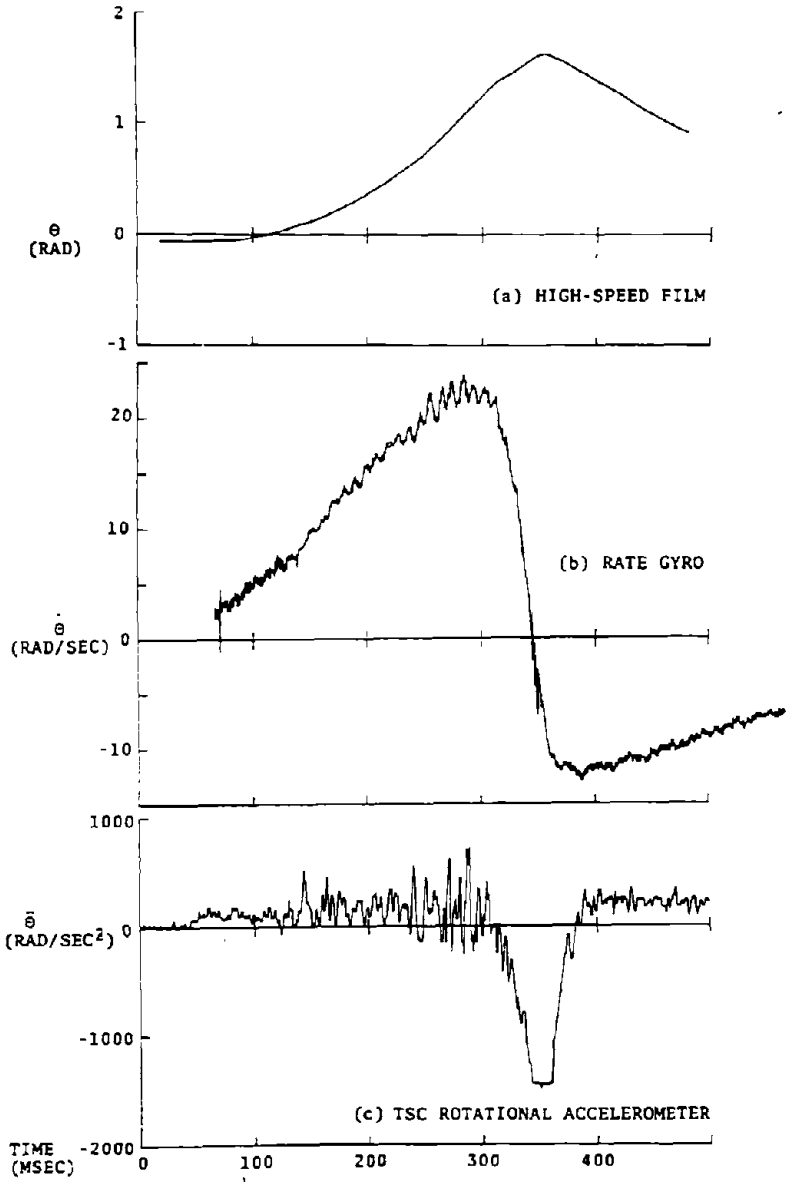

Figure 5. Directly Measured Data Obtained in one NADC Run.

directly from the output of the computer plotter.

The outputs of the two rotational accelerometers (TSC and Navy) were quite similar, so only the TSC accelerometer data is shown here for the angular acceleration, $\ddot{\theta}$. The "squared-off" portion of the signal at approximately t = 350 msec was not in the accelerometer output signal; the gain of the attached amplifier was too high and the resulting voltage saturated the input of the tape recorder. This large negative acceleration occured when the dummy's chin struck its stop and rebounded sharply. The small rapid variations in $\ddot{\theta}$ are due to the noise present in the system and include both mechanical vibration picked up by the accelerometer, and electrical disturbances.

To compare and validate the data from various sources, it was next necessary to convert to one common property of motion. The computer was used to perform the necessary transformations. As shown in Figure 6, the film data was differentiated and the accelerometer data was integrated. Note that the noise was such that

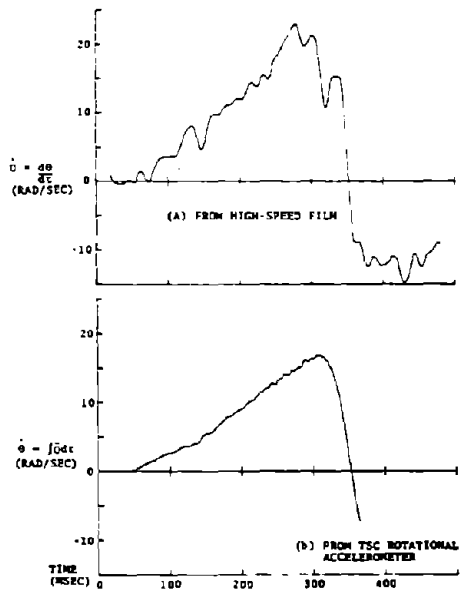

Figure 6. Derived Data Obtained in One NADC Run.

differentiation tended to exaggerate it and integration tended to smooth it. This was expected and indicates the limited usefulness of film data. Also note that the integration of angular acceleration was terminated at the point where the saturation occured, to avoid misleading conclusions.

The curves which show angular velocity, $\dot{\theta}$, (Figure 5b, Figure 6a, Figure 6b) are shown superimposed in Figure 7. They are quite similar, with a gradually increasing positive angular velocity followed by a sudden large negative angular velocity where the dummy head's chin struck and rebounded. The most noticeable discrepancy (neglecting noise in the signals) is the lower magnitude of the angular velocity as derived from the accelerometer. This is a result of the limited low frequency response of the accelerometer. The missing frequency component of angular acceleration reduces the value of the integral $\int \ddot{\theta}\, dt$.

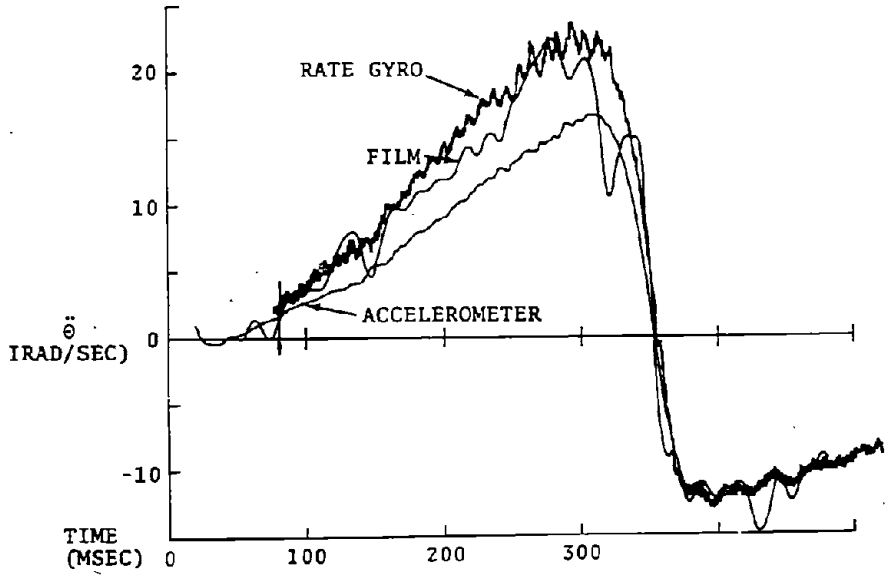

Figure 7. Comparison of Results Obtained with Different Instruments in one NADC Run.

5.0 FIELD TEST (HUMANS)

The first field tests of the rotational accelerometer using human subjects were conducted at the Daisy test track facility at Holloman AFB New Mexico. The tests were: (1) to solve any problems in integrating the accelerometer system with the rest of the Holloman instrumentation; (2) to determine the required channel capacity of the recording electronics, i.e. amplitude and frequency response; and (3) to correlate the accelerometer data with the photographic data.

Figure 8 is a photograph of the subject strapped into the seat on the sled. The rotational accelerometer was in his mouth and its lead routed out between his lips and along his chin. There was no shoulder harness, so as the sled decelerated his upper torso was free to swing forward while his hips were held by the lap belt. The test accelerations were in the 5g to 7g range. A high-speed camera was set up beside the test track (but not on the

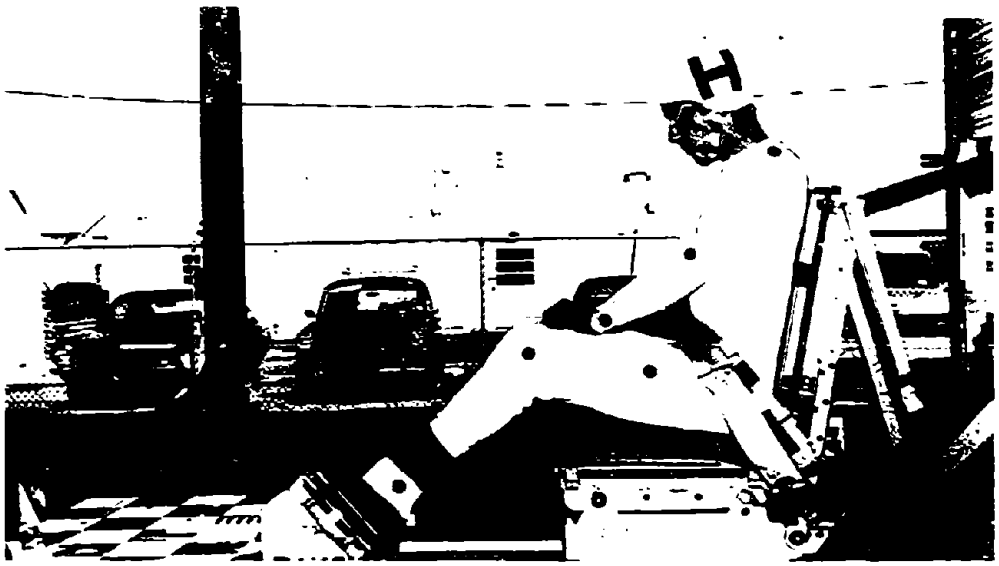

Figure 8. Holloman Test Configuration

sled) to measure angular position. There was no device for direct measurement of angular velocity.

Figure 9a contains the raw data from the accelerometer for one run. The many small, rapid fluctuations and the occasional spikes are noise in the system. To determine how much filtering was needed, the Fourier spectrum of the data was taken, as shown in Figure 9b. The largest frequency components occur at low frequencies, as expected. Up to approximately 100 Hz, the frequency components roll-off at a rate of 20 dB/decade; beyond 100 Hz they stay relatively constant. This high frequency behavior is characteristic of noise, as expected, with a signal-to-noise ratio of approximately 40 dB, or 100:1. Therefore, the raw data was filtered on the computer with a Gaussian Filter* with half-power point of 100 Hz. The filtered data is shown in Figure 9c.

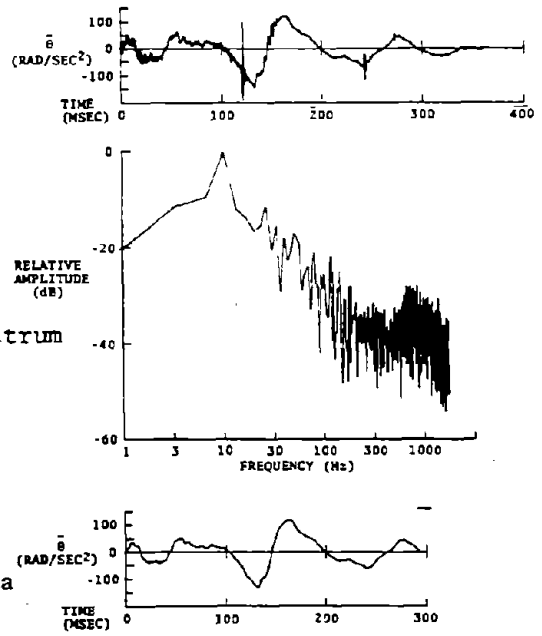

Figure 9. Rotational Accelerometer Data Obtained in One Run at Holloman AFB

*Report No. DOT-TSC-NHTSA-71-4, p. 31

Figure 10 contains the filtered data from the high-speed film for the same run. This data had to be filtered with half-power point of 20 Hz. The camera was not on board the sled, and the subject was restrained by only a lap belt. The film data, therefore, was not purely rotational, as at Johnsville, but contained a large translational component. The cursor of the film reader had to be moved many times to track the subject. This operation adds a large amount of noise to the data.

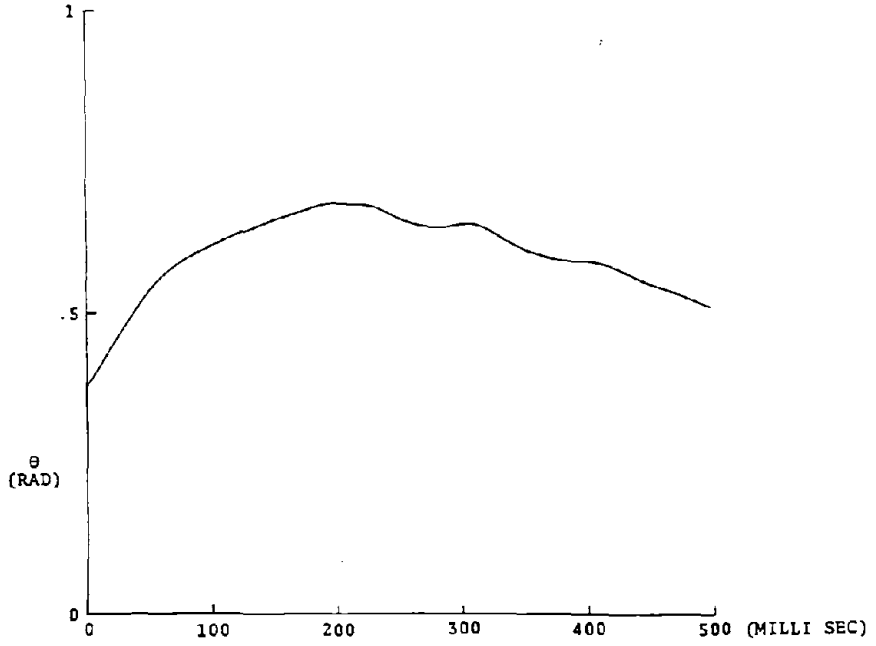

Figure 10. High Speed Film Data Obtained in One Run at Holloman AFB

Figure 11 illustrates the two derived curves for angular velocity in this experiment. It is obvious that they have few common characteristics. There could be several explanations for this. The filtering of the data for the angle, θ, at 20 Hz may have removed too much of the signal along with the noise. The large translational component of the motion may have introduced spurious signals in the accelerometer; this is discussed in detail in section 3.0. Also, the fairly small size of the target on the film made alignment of the cursor difficult and imprecise. Many

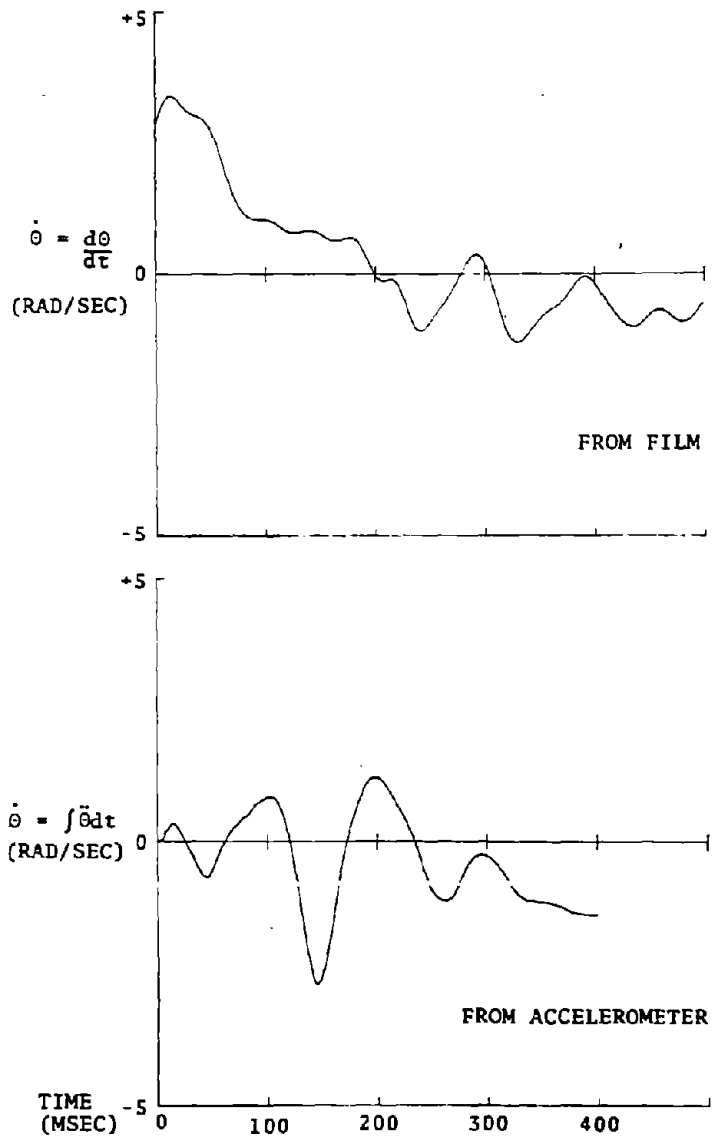

Figure 11. Derived Data Obtained in One Run at Holloman AFB

of these difficulties were expected; with the development of an accelerometer less susceptible to translation and with the use of an on-board camera with a better target, results similar to those from Johnsville should be obtained.

6.0 CONCLUSIONS & RECOMMENDATIONS

Laboratory and field tests have shown the miniature mouthpiece rotational accelerometer to be an accurate reliable device for measuring purely rotational head accelerations. However when high linear accelerations are encountered the device can give an ambiguous output. That is to say, from the accelerometer output alone one cannot be sure whether it is responding to linear or rotational accelerations. To determine the rotational acceleration, the linear acceleration must be known. Then by referring to the equation in figure 2 the rotational acceleration can be determined. The linear component can be most easily found by the installation of a triaxial linear accelerometer alongside the rotational accelerometer. This technique is currently being field tested. Another promising technique for the determination of the rotational acceleration would employ a six accelerometer package as a sensor. The six linear accelerometers would be mounted on the faces of a cube and measure the accelerations about and along the three mutually perpendicular axis through the center of the cube and perpendicular to its faces. Such a device has been designed and a vendor found to fabricate a prototype model.

APPENDIX A

DETERMINATION OF COEFFICIENTS OF ROTATIONAL COMPONENT

APPENDIX A

DETERMINATION OF COEFFICIENTS OF ROTATIONAL COMPONENT

The overall calibration setup is shown in Figure A-1. The relationship between rotational acceleration and tangential linear acceleration is:

$$\ddot{r} = R\,\ddot{\theta}$$

where R is the radius of curvature. Referring to the coordinate system shown previously, the total output of the device is:

$$\text{output} = a\,\ddot{\theta}_x + b\,\ddot{\theta}_y + c\,\ddot{\theta}_z + d\,\ddot{r}_x + e\ddot{r}_y + f\ddot{r}_z$$

The coefficients d, e and f are easily determined by vibrating the device linearly on each axis.

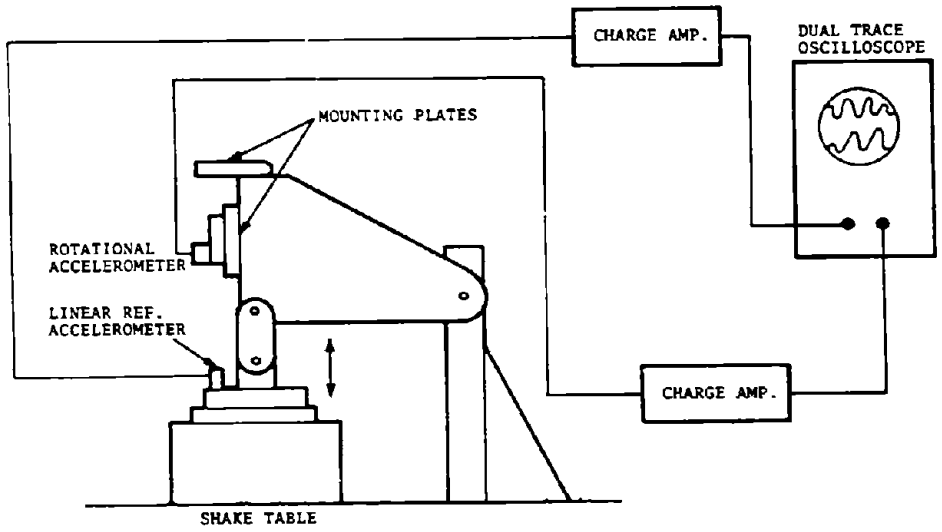

Figure A-1. Calibration Setup

Because the calibration jig was not specifically designed to vibrate in modes that would make it easy to determine the coefficients for the rotational components, certain calculations had to be made. The geometry of the calibration fixture is shown in Figure A-2. If the transducer is mounted on mounting plate A it can easily be shown that:

$$\ddot{r}_3 = \ddot{r}_1$$

$$\ddot{r}_4 = .5\ \ddot{r}_1$$

$\ddot{r}_1$ is the linear acceleration of the shake table and is measured by a "standard" linear accelerometer. If the transducer is mounted on mounting plate B we have:

$$\ddot{r}_3 = \ddot{r}_1$$

$$\ddot{r}_4 = .236\ \ddot{r}_1$$

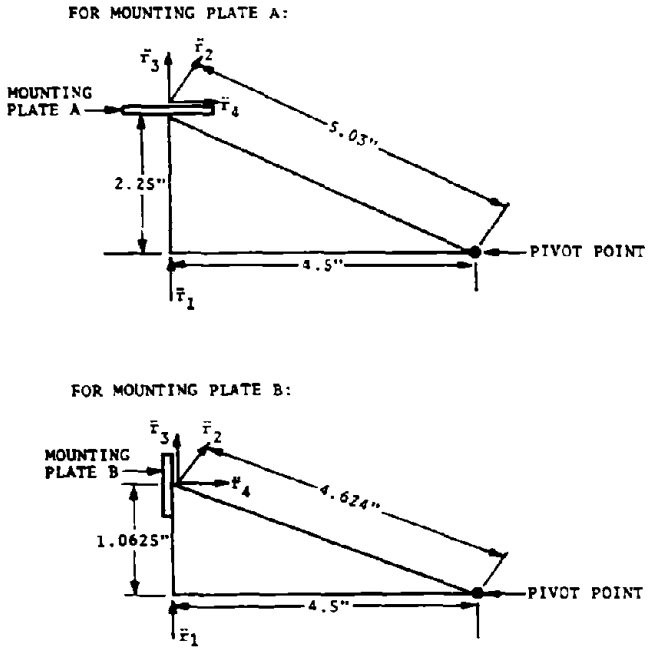

Figure A-2. Geometry of Calibration Fixture

These relationships must be considered in determining the rotational coefficients. The various vibrational modes used in the calibration are illustrated in Figure A-3. Other modes may also be used but these are adequate to determine the six coefficients. The three coefficients for the linear components can be found directly by vibrating in modes (1), (2), and (3).

To determine the coefficient "a" we can vibrate in mode (4). In mode (4) we have:

$$Q_{out} = a\,\ddot{\theta}_x + e\ddot{y} + f\ddot{z}$$

$\ddot{\theta}_x$, $e\ddot{y}$ and $f\ddot{z}$ are known and a is solved.

To determine coefficient "b" we use modes (8) and (9). In mode (8) we have:

$$Q_{out} = b\,\ddot{\theta}_y - d\ddot{x} - f\ddot{z}$$

In mode (9) we have:

$$Q_{out} = -\,b\,\ddot{\theta}_y + d\ddot{x} - f\ddot{z}$$

The difference is

$$Q_{out}\ (diff) = -\,2b\,\ddot{\theta}_y + 2\,d\ddot{x}$$

$\ddot{\theta}_y$, and $d\ddot{x}$ are known and "b" is solved.

To determine coefficient "c" we use modes (6) and (7). In mode (6) we have:

$$Q_{out} = c\ddot{\theta}_z - d\ddot{x} + e\ddot{y}$$

In mode (7) we have:

$$Q_{out} = c\ddot{\theta}_z + d\ddot{x} - e\ddot{y}$$

The sum is

$$Q_{out}\ (sum) = 2c\ddot{\theta}_z$$

$\ddot{\theta}_z$ is known and "c" is solved.

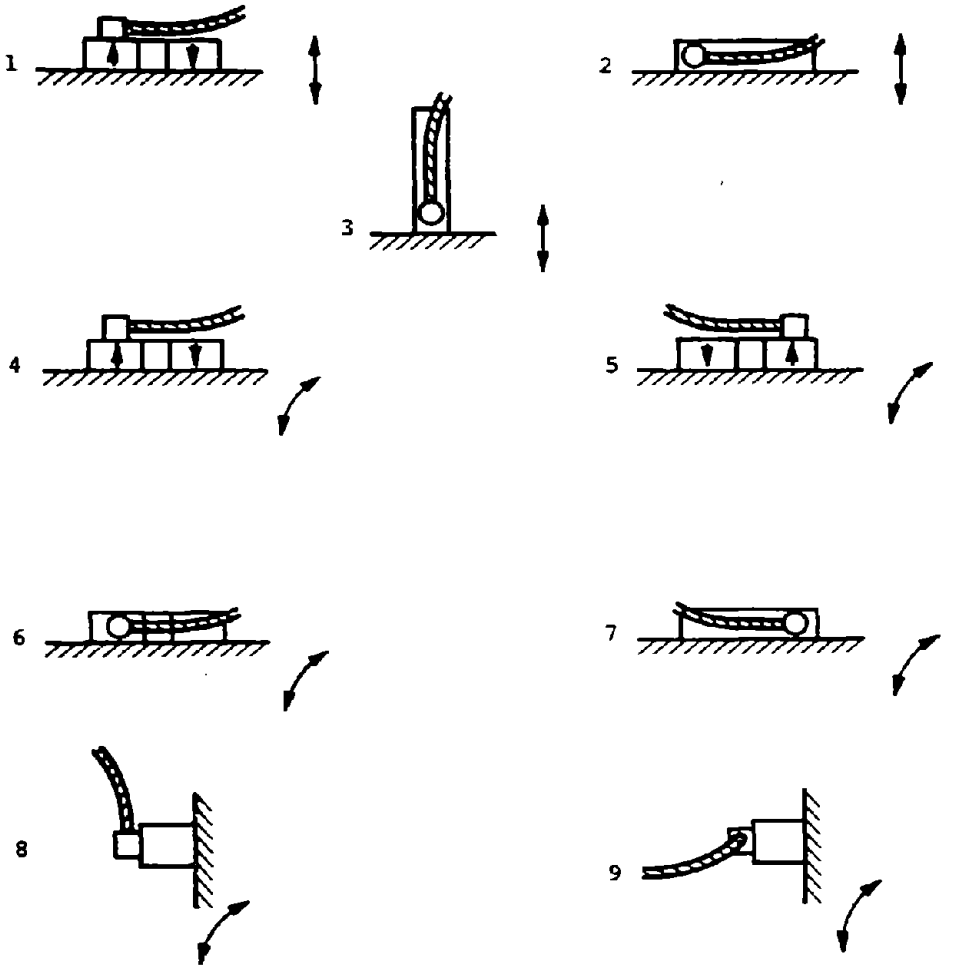

Figure A-3. Vibrational Modes Used in Calibration

DEMONSTRATION OF SUPERPOSITION

The superposition of linear and rotational outputs can be shown by vibrating the accelerometer in modes (4) and (5). In mode (4) we have:

$$Qout = a\ddot{\theta}_x + e\ddot{y} + f\ddot{z}$$

In mode (5) we have:

$$Qout = - a\ddot{\theta}_x - e\ddot{y} + f\ddot{z}$$

The sum is:

$$Qout\ (sum) = 2f\ddot{z}$$

$2f\ddot{z}$ is known from the linear vibrational modes and is exactly the sum of the outputs for modes (4) and (5).

78179